Loss of cathepsin C enhances keratinocyte proliferation and inhibits apoptosis

Xin Li, Ling-Fei Jia, Yunfei Zheng, Yiping Huang, Man Qin & Yuan Yang

Science Bulletin

ISSN 2095-9273
Volume 61
Number 14

Sci. Bull. (2016) 61:1107-1114
DOI 10.1007/s11434-016-1085-z

Springer

Sci. Bull. (2016) 61(14):1107–1114
DOI 10.1007/s11434-016-1085-z

www.scibull.com
www.springer.com/scp

Article

Life & Medical Sciences

Loss of cathepsin C enhances keratinocyte proliferation and inhibits apoptosis

Xin Li · Ling-Fei Jia · Yunfei Zheng · Yiping Huang · Man Qin · Yuan Yang

Received: 24 December 2015 / Revised: 21 February 2016 / Accepted: 31 March 2016 / Published online: 11 June 2016

Abstract Papillon–Lefèvre Syndrome is a rare autosomal recessive disorder characterized by rapidly progressive periodontitis and confined palmoplantar hyperkeratosis resulting from genetic mutations in *cathepsin C* (*CTSC*). The present study investigated the effect of CTSC on keratinocyte proliferation and apoptosis. HaCaT keratinocytes were transfected with wild-type *CTSC* and *CTSC*-targeted siRNAs to investigate the effects of CTSC expression on cell keratosis. Real-time PCR and Western blot analyses showed that the levels of loricrin and keratin (KRT)-1, but not KRT9, was correlated with CTSC expression. Loricrin was increased in the CTSC-overexpression group and downregulated in the *CTSC*-silenced group. A positive association between loricrin expression and cell apoptosis was detected in HaCaT keratinocytes. KRT1 was decreased in the CTSC-overexpression group and increased in the *CTSC*-silenced group. Prominent, punctuate KRT1 aggregates were present in *CTSC*-knockdown HaCaT cells. This study suggested that loss of CTSC contributes to keratinocyte hyperkeratosis via downregulation of loricrin and enhanced cell proliferation.

Keywords Papillon–Lefèvre syndrome · Cathepsin C · Loricrin · Cytokeratin 1 · Cytokeratin 9

1 Introduction

Papillon–Lefèvre syndrome (PLS, MIM 245000) is a rare autosomal recessive disorder characterized by rapidly progressive periodontitis and palmoplantar keratoderma [1]. The PLS gene was found to be located on chromosome 11q14 by homozygosity mapping [2, 3]. This mapped region contains the causative *cathepsin C* (*CTSC*) gene [4, 5], which encodes the CTSC protein, an activator of the serine proteinases elastase, cathepsin G and proteinase 3, in polymorphonuclear cells (PMNs) [6]. PMN-derived serine proteinases play a salient role in the immune system, and their absence in patients with PLS is consistent with their vulnerability to periodontal infection [6]. Therefore, mutations in CTSC are associated with a higher risk of infections [7, 8]. The clinical epidermal symptoms indicate that CTSC is associated with cell differentiation or epidermal cornification; thus, *CTSC* gene mutations may be responsible for other hereditary epidermal diseases involving hyperkeratosis [9]. However, the role of CTSC in keratoderma hyperkeratosis remains unclear.

The palmoplantar keratodermas are a group of disorders characterized by hyperkeratosis of the palms and soles; however, the etiology is highly heterogeneous and complex

Xin Li and Ling-Fei Jia contributed equally to this work.

X. Li · M. Qin · Y. Yang (✉)
Department of Pediatric Dentistry, Peking University School and Hospital of Stomatology, Beijing 100081, China
e-mail: rubyea@sina.com

L.-F. Jia · Y. Zheng
Department of Oral and Maxillofacial Surgery, Peking University School and Hospital of Stomatology, Beijing 100081, China

L.-F. Jia
Central Laboratory, Peking University School and Hospital of Stomatology, Beijing 100081, China

Y. Huang
Department of Orthodontics, Peking University School and Hospital of Stomatology, Beijing 100081, China

[10]. The disease-causing gene was first localized to the *type I keratin* (*KRT*) gene cluster, which includes the *KRT9* gene [11]. Many *KRT9* mutations have been identified in families with epidermolytic palmoplantar keratoderma (EPPK) in different populations [12, 13]. Several mutations in the *KRT1* gene lead to a phenotype that can be difficult to distinguish clinically and histologically from EPPK [14–17]. In addition, loricrin is associated with hyperkeratosis. HaCaT keratinocytes transfected with wild-type loricrin were susceptible to programmed cell death (PCD) [18]. During terminal cornification differentiation of keratinocytes, the plasma membrane is replaced by loricrin, which is highly abundant in the cornified layer [19]. Mutations in the loricrin gene underlie certain congenital epidermal abnormalities including hyperkeratosis of the palms and soles with digital constriction, which are typically detected [20]. Thus, KRT9, KRT1 and loricrin are suspected to be involved in PLS, as these genetic abnormalities are associated with similar skin lesions.

In 2007, we reported two novel mutations in *CTSC* in two Chinese patients with PLS [21]. This study further investigated CTSC and its relationship with KRT1, KRT9 and loricrin. Our findings suggested that *CTSC* loss-of-function enhanced HaCaT keratinocyte proliferation and KRT1 upregulation which shed light on the pathogenesis of PLS and the role of *CTSC* loss-of-function mutations in clinical manifestation.

2 Materials and methods

2.1 *CTSC* expression and RNA oligoribonucleotide constructs

A wild-type human *CTSC* vector was constructed by subcloning full-length cDNA into the pcDNA3.1 plasmid (Invitrogen, Carlsbad, CA, USA). Small interfering (si) RNAs (siRNA-1 and siRNA-2) targeting the human *CTSC* transcript and a scramble control were designed (Table 1). Both the *CTSC* constructs and siRNAs were purchased from Integrated Biotech Solutions Company (Ibsbio Co., Shanghai, China).

2.2 Keratinocyte culture and transfection

HaCaT cells (American Type Culture Collection, ATCC; Manassas, VA, USA) were cultured in Dulbecco's Modified Eagle's Medium (DMEM) supplemented with 10 % fetal bovine serum (FBS). HaCaT cells were plated at a density of 1.0×10^5/well in six-well plates and, upon reaching 80 % confluency, were transfected using Lipofectamine 2000 (Invitrogen) with 4.0 μg pcDNA3.1 empty vector or pcDNA3.1-*CTSC* and 100 nmol/L siRNA-1, siRNA-2, or scrambled siRNA. An additional well was transfected with pcDNA3.1-*GFP* control vector to assess the transfection efficiency.

2.3 Real-time PCR

At 24 h post-transfection, total mRNA was extracted from HaCaT cells using TRIzol reagent (Invitrogen); the mRNA was then reverse transcribed into cDNA. Quantitative PCR was performed using the ABI Prism 7500 Real-time PCR System (Applied Biosystems). The amplification procedure consisted of 10 min at 95 °C followed by 40 cycles of 15 s at 95 °C and 1 min at 60 °C. Primer sequences are listed in Table 1. Relative mRNA expression levels were determined by the comparative threshold method.

2.4 Western blotting and data analysis

Western blot was performed as described previously [22]. At 48 h post-transfection, cell lysates were collected to extract protein. Equal volumes of the extracted proteins were loaded onto SDS polyacrylamide gels, transferred onto nitrocellulose membranes, and analyzed using antibodies. GAPDH was probed as a loading control where appropriate. The primary antibodies against CTSC,

Table 1 Sequences of RNA oligonucleotides

Name	Sense strand primer (5′–3′)	Antisense strand primer (5′–3′)
siRNA duplexes		
Scrambled	UUC UCC GAA CGU GUC ACG UTT	ACG UGA CAC GUU CGG AGA ATT
siRNA-1	GCA ACU ACA UAC AUG GAA UTT	AUU CCA UGU AUG UAG UUG CTT
siRNA-2	GCU ACU CAU UUG CUU CUA UTT	AUA GAA GCA AAU GAG UAG CTT
Real-time PCR primers		
CTSC	ATG TCA ACT GCT CGG TTA TGG G	AAG CCT TGG TTG TAA ATG ATG GTG
Loricrin	GGA GTT GGA GGT GTT TTC CA	ACT GGG GTT GGG AGG TAG TT
KRT1	ATC AAT CTC GGT TGG ATT CG	TCC TGC TGC AAG TTG TCA AG
KRT9	GCC TGC TTA TTG GAT CCT GA	CAG GCC AGA GAG AGG AAA GA

loricrin, KRT1, KRT9 and GAPDH were purchased from Santa Cruz Biotechnology Inc. (Santa Cruz, CA, USA). Protein densitometry was performed using ImageJ software (http://rsb.info.nih.gov/ij/); protein band densities were quantified and normalized to that of GAPDH.

2.5 CTSC enzymatic activity

CTSC activity was determined by measuring the amount of 7-amino-4-methylcoumarin (AMC) released by hydrolysis of the synthetic substrate glycyl-L-arginine-AMC (AMC, Ibsbio Co., Ltd., Shanghai, China). Briefly, cell lysates (20 μL) were added to 200 μL phosphate-buffered saline (PBS, 0.1 mol/L, pH 6.5) containing glycyl-L-arginine-AMC (0.5 mmol/L), NaCl (2 mmol/L) and dithiothreitol (2 mmol/L) (Biomart, Shanghai, China). The reactions were then incubated at 37 °C for 30 min followed by the addition of 1 mL glycine–NaOH buffer (0.5 mol/L, pH 9.8) to terminate the reaction. Fluorescence was monitored using a fluorescence spectrophotometer (Bio-Tek Instruments Inc., Winooski, VT, USA) at an excitation wavelength of 370 nm and an emission wavelength of 460 nm. Enzymatic activity was calculated by converting fluorescence to activity using AMC standards. Activity is expressed as nmol AMC produced in 1 h by 1 mg cell lysate [23].

2.6 Confocal immunofluorescence

At 48 h post-transfection, HaCaT cells were washed with PBS, fixed with 4 % paraformaldehyde, permeabilized with 0.1 % Triton X-100, and then blocked with 5 % FBS in PBS. CTSC was detected using a monoclonal antibody that binds to the heavy chain of CTSC (Santa Cruz) and fluorescein-conjugated AffiniPure goat anti-mouse IgG secondary antibody (Invitrogen). KRT1 was detected with monoclonal anti-cytokeratin 1 antibody (Santa Cruz) and fluorescein-conjugated AffiniPure goat anti mouse IgG. The cell skeleton was detected using a monoclonal anti-tubulin antibody (ab18251; Abcam, Cambridge, MA, USA) and rhodamine-conjugated AffiniPure goat anti-rabbit IgG. Cells were stained with 4′,6-diamidino-2-phenylindole (DAPI) to visualize the nucleus and then mounted onto slides. Cells were examined using a confocal laser-scanning microscope.

2.7 Cell proliferation and apoptosis

The Cell Counting Kit-8 (CCK-8, Dojindo, Kumamoto, Japan) was used to measure the effects of CTSC overexpression and knockdown on the proliferation of HaCaT cells. HaCaT cells were grown in 96-well plates (2×10^3/well) for 24 h and then transfected with pcDNA3.1-CTSC or CTSC siRNAs. CCK-8 (10 μL) was added to each well at 0, 24, 48 and 72 h post-transfection and incubated at 37 °C for 2 h; a microplate reader (Bio-Tek Instruments Inc., Winooski, VT, USA) was used to measure the absorbance at 450 nm.

To further measure keratinocyte apoptosis, a TdT-UTP nick end labeling (TUNEL) assay kit (Beyotime Institute of Biotechnology, Jiangsu, China) was used to label the 3′-end of fragmented DNA from apoptotic cells. At 24 h post-transfection, cells were washed with PBS, fixed with 4 % paraformaldehyde for 30 min, and then permeabilized with 0.1 % Triton X-100 at 4 °C for 2 min. The TUNEL reaction mixture was added to each sample and incubated at 37 °C in the dark for 1 h. Cells were imaged with a fluorescence microscope to identify apoptotic cells, as indicated by red fluorescence.

The Apo-ONE Homogeneous Caspase-3/7 Assay kit (Promega, USA) was used to detect caspase-3/7 activity in accordance with the manufacturer's protocol. At 24 h post-transfection, 100 μL of the blank, the control or cells were incubated with 100 μL Apo-ONE Caspase-3/7 Assay reagent in 96-well microtiter plates at 37 °C for 2 h. Caspase-3/7 activity was measured by fluorescence emission at an excitation wavelength of 499 nm and an emission wavelength of 521 nm. Data are presented as mean ± SD from three independent experiments.

3 Results

HaCaT cells were transiently transfected with *CTSC* constructs and siRNAs. The transfection efficiency was >70 % after 48 h (Fig. 1a). The *CTSC* mRNA level in the CTSC-overexpression group was 12-fold higher than that in the control group. In contrast, the mRNA level in the CTSC-silenced group was 20 % of that expressed by the control (Fig. 1b). Western blot analysis showed that the CTSC protein expression levels coincided with the mRNA expression (Fig. 1c, d). CTSC activity was increased in cells overexpressing CTSC but reduced in cells transfected with siRNA-1 and siRNA-2 ($^*P < 0.05$) (Fig. 1e).

3.1 CTSC knockdown caused aggregation of keratin filaments

Under microscopy, CTSC localization was dispersed in the cytoplasm of HaCaT cells. At 48 h post-transfection, cells overexpressing CTSC showed a higher density of CTSC than that of cells expressing empty vector (pcDNA3.1). As expected, CTSC density was decreased in cells transfected with siRNAs compared with cells expressing scrambled siRNA (Fig. 2).

At 48 h post-transfection, the majority of cells transfected with scrambled siRNA, pcDNA3.1 or CTSC

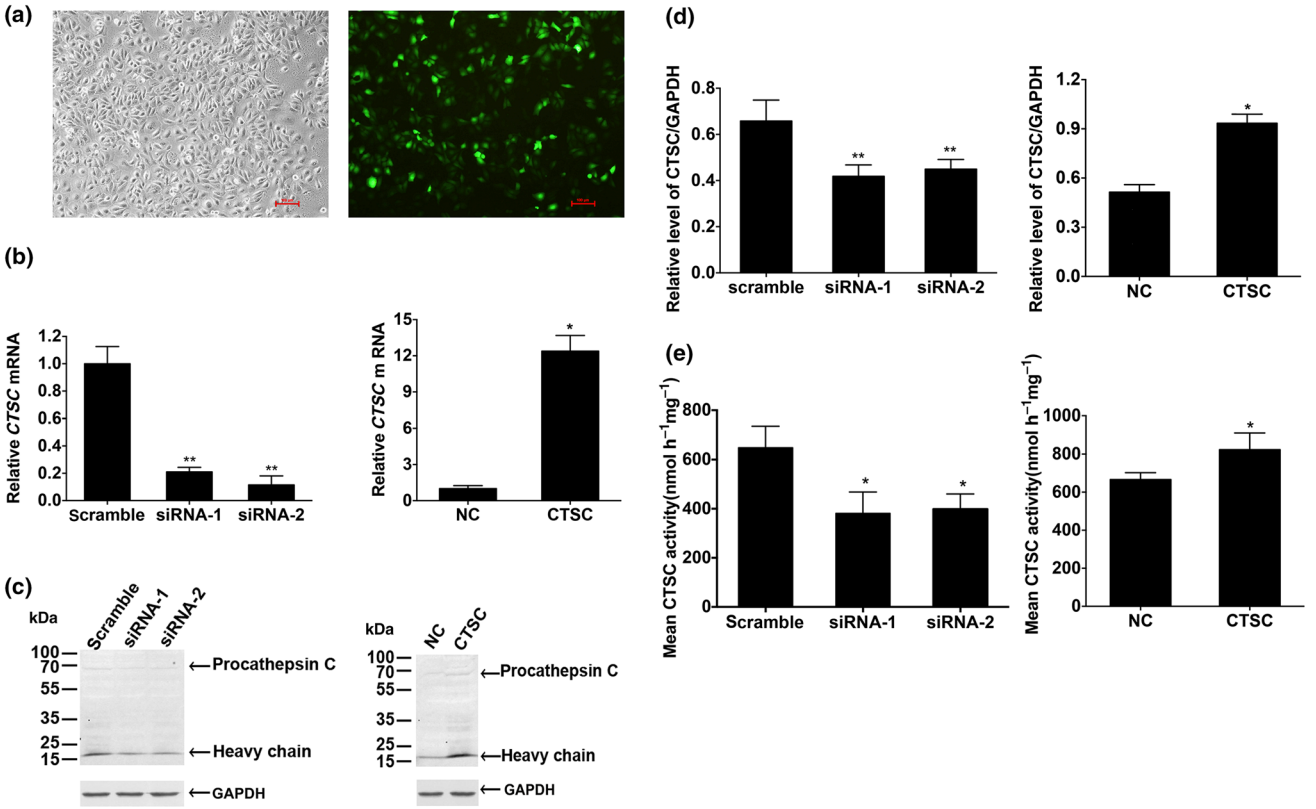

Fig. 1 (Color online) HaCaT cells were transiently transfected with *cathepsin C* (*CTSC*) gene constructs and small interfering (si)RNAs. **a** The transfection efficiency using pcDNA3.1-*GFP* control vectors was >70 % at 48 h post-transfection. **b** The *CTSC* mRNA level was 12-fold higher in the CTSC-overexpression group and 20 % lower in the CTSC-silenced groups compared with levels in the controls. **c** Western blot analysis of CTSC protein in cells transfected with scrambled siRNA, siRNA-1, siRNA-2, pcDNA3.1 (NC) and *CTSC*. GAPDH was an internal marker for equal protein loading amounts. **d** Densitometric analysis of three separate experiments. Data are presented as mean ± SD (**$P < 0.01$). **e** CTSC activity was increased in CTSC-overexpressing cells but reduced in CTSC-silenced cells (*$P < 0.05$)

constructs had morphologically normal keratin filaments (Fig. 2f, i, j). When CTSC was knocked down using siRNA-1 and siRNA-2, small, irregular and densely stained punctate aggregates were detected in some HaCaT cells (Fig. 2g, h).

3.2 Overexpression of CTSC in HaCaT cells inhibited cell proliferation and promoted apoptosis

Overexpression of CTSC inhibited the viability of HaCaT cells (Fig. 3a). CTSC knockdown promoted cell proliferation at 24, 48 and 72 h post-transfection. TUNEL reactivity was clearly detected at 24 h post-transfection. As shown in Fig. 3b, silencing of *CTSC* significantly reduced apoptosis in HaCaT cells, and overexpression of CTSC significantly induced apoptosis. The CTSC overexpression group showed 20.42 % apoptotic cells in the CTSC overexpression group compared with 10.87 % in the control group. TUNEL positivity was detected in 5.7 % and 6.1 % of HaCaT cells in *CTSC* siRNA-1 and siRANA-2 knockdown groups, respectively, compared with 10.7 % in the scrambled group (Fig. 3c).

Caspase-3/7 plays a vital role during the execution phase of cell apoptosis; therefore, we tested whether CTSC overexpression increased caspase-3/7 activation. As shown in Fig. 3d, caspase-3/7 activation was increased significantly in the CTSC-overexpression group compared with the control group. Caspase-3/7 activation was dramatically reduced in the CTSC-silenced groups compared with the control group.

3.3 Effects of *CTSC* transfection on *loricrin*, *KRT1* and *KRT9* expression

To characterize the molecular basis for the effects of *CTSC* expression on cell keratosis in HaCaT cells, the expression of key cell keratosis-related proteins, loricrin, KRT1 and KRT9, was examined.

The expression of loricrin and *KRT1* mRNA, but not *KRT9*, correlated with *CTSC* expression. Expression of

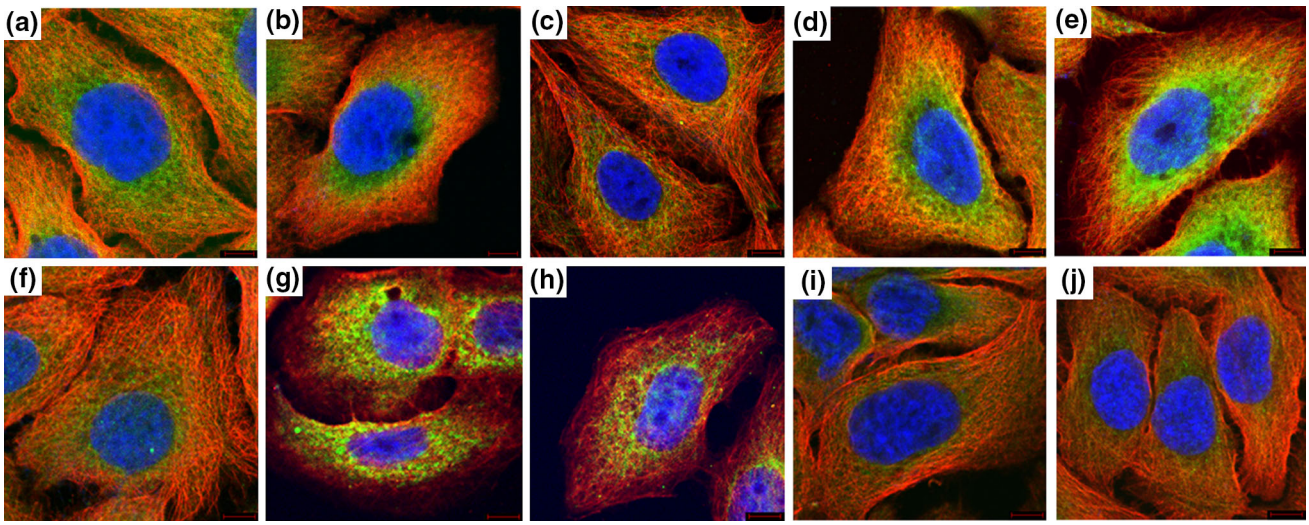

Fig. 2 Visualization of HaCaT cells using confocal laser scanning microscopy; the blue signal indicates the cell nucleus stained by DAPI, the red signal indicates tubulins, and the green signal indicates CTSC (**a**–**e**) and KRT1 (**f**–**j**). Microscopy showed that CTSC was dispersed in the cytoplasm of HaCaT cells. At 48 h post-transfection, siRNA-1- and siRNA-2-transfected cells (**b**, **c**) showed less intensive CTSC signals compared with scrambled siRNA-transfected cells (**a**). In contrast, CTSC-overexpressing cells (**e**) showed a higher CTSC density than that of pcDNA3.1 empty vector-expressing cells (**d**). Overexpression or silencing of CTSC had no effect on the cytoskeleton of HaCaT cells at 48 h post-transfection. **f** Keratin filaments with essentially normal morphology were observed in cells transfected with scrambled siRNA (**g**, **h**) Cells with prominent, punctuate KRT1 aggregates were present in siRNA-1- and siRNA-2-transfected cells. **i**, **j** Cells transfected with pcDNA3.1 vectors and *CTSC* constructs presented normal keratin filaments as in the scrambled siRNA group

loricrin mRNA was positively correlated with *CTSC* expression in HaCaT cells (Fig. 4a). *KRT1* mRNA was decreased in the CTSC-overexpression group and increased in the *CTSC*-silenced group (Fig. 4b). The expression of KRT9 showed little change in the CTSC-overexpression or -silenced groups (Fig. 4c). Western blot showed that loricrin, KTR1 and KRT9 protein levels were consistent with mRNA expression levels (Fig. 4d, e).

4 Discussion

Previously, we reported two novel mutations of the *CTSC* gene in two Chinese patients with PLS [21]. So far, 75 disease-related mutations have been reported in the *CTSC* gene; however, genotype–phenotype correlations have not yet been identified by *CTSC* gene mutation comparisons [24]. Keratinization has been regarded as a specialized form of apoptosis or PCD. From the basal layer to the superficial stratum corneum, keratinocytes proliferate, differentiate and undergo apoptosis and are sequentially replaced by succeeding cells. The desquamation rate of cells in the stratum corneum has to be in precise balance with the proliferation rate of cells in the basal layer to maintain a normal epidermis [25]. Mutations in genes that encode cornified cell envelope proteins, enzymes and their inhibitors are most likely to cause inherited keratinizing disorders, since these proteins play fundamental roles regulating cell differentiation, proliferation and adhesion [26].

The present study investigated the pathogenesis of PLS, from the genotypic cause to the clinical manifestation. We showed that when *CTSC* was silenced in HaCaT cells, proliferation was promoted. As the proliferation-desquamation balance was disrupted, keratinocytes with abnormal desquamation accumulated, leading to keratoderma hyperkeratosis.

In vitro, a mutation in the L12 domain of keratin 1, a keratin skeleton protein, was found to be associated with mild epidermolytic ichthyosis. The percentage of cells with keratin aggregates and an abnormal keratin skeleton increased dramatically in HaCaT cells expressing mutant *KRT1* compared with cells expressing wild type *KRT1* [27]. When *CTSC* was silenced KRT1 was upregulated at the mRNA and protein levels. However, other than the observed keratin aggregates, the cytoskeletal network exhibited normal morphology. These results are consistent with a *KRT1* S233L mutation in domain 1B [28]. We believe these observations are due to differences in morphology and gene expression of cells cultured in vitro compared with cells that in multilayered epidermis in vivo.

This study demonstrated that activation of caspase-3/7 accompanied cell apoptosis when CTSC was overexpressed in HaCaT keratinocytes. Whereas silencing of *CTSC* inhibited cell apoptosis and casapse-3/7 activation.

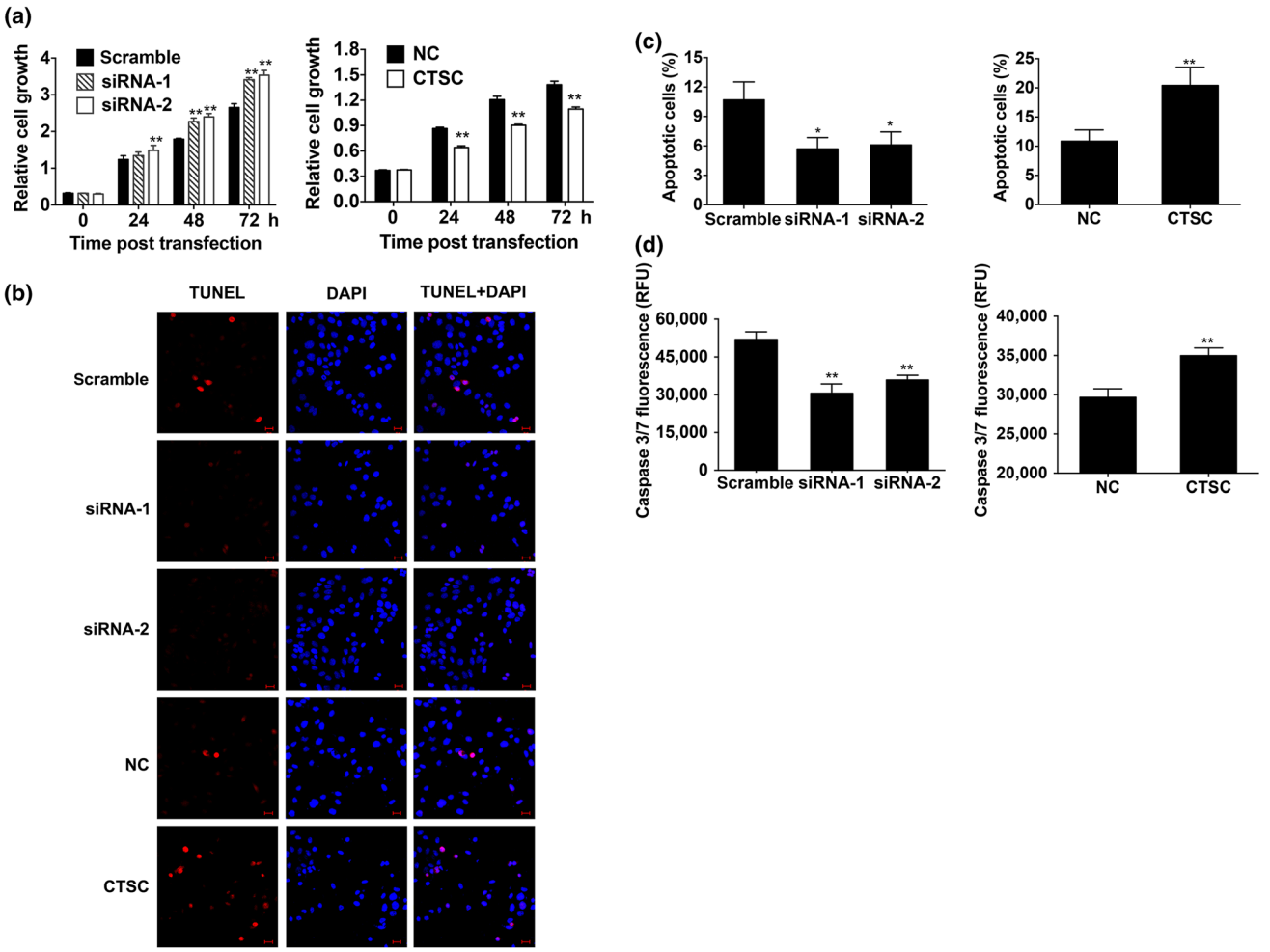

Fig. 3 CTSC overexpression in HaCaT cells inhibited cell proliferation and promoted apoptosis. **a** Transfection with *CTSC* siRNAs significantly increased cell numbers compared with transfected with scrambled siRNA at 48 and 72 h post-transfection. Transfection with CTSC constructs at for 24, 48 and 72 h significantly decreased cell numbers compared with transfection with pcDNA3.1. Data are presented as mean ± SD (**$P < 0.01$). **b** TdT-UTP nick end labeling (TUNEL) showed that apoptosis occurred in HaCaT cells transfected with siRNAs, *CTSC* constructs and scrambled siRNA. **c** 4′,6-diamidino-2-phenylindole (DAPI)-positive cells were counted in five random microscopic fields, and the mean percentage of apoptotic cells was expressed as mean ± SD (*$P < 0.05$, **$P < 0.01$). When HaCaT cells were transfected with siRNAs, 5.7 % and 6.1 % of cells were TUNEL-positive, respectively, in the two groups compared with 10.7 % in the scrambled siRNA group. The CTSC-overexpression group showed 20.42 % apoptotic HaCaT cells compared with 10.87 % in the control group. **d** Caspase-3/7 activation was increased significantly in the CTSC-overexpression cells, compared with the control. In contrast, caspase-3/7 activation was reduced significantly in the CTSC-silenced groups, compared with the control. Data are presented as mean ± SD (**$P < 0.01$)

In addition, loricrin expression was upregulated when CTSC was overexpressed and downregulated when *CTSC* was silenced. These effects are in accordance with previous finding that wild type loricrin upregulation in HaCaT keratinocytes induced PCD and caspase-14 activation [18]. Moreover, in vivo, TUNEL-positive cells were increased in the skin of patients with loricrin keratoderma [20]. However, when loricrin was overexpressed in a transgenic mouse model, there was no evidence of a disease-associated phenotype [29]. Although water-barrier function was slightly weakened 5 d after birth, null mice had no distinct abnormalities in the absence of loricrin [30]. The authors speculated that the lacking of phenotype in vivo was due to increased resistance to keratin deficiency due to enhanced level of keratins in the epidermis. Together with desmosomes that anchor keratinocytes, kermatins form a complex intermediate filament network. In contrast, cultured monolayer cells are more vulnerable to keratin filament disruption.

In this study, KRT1 and loricrin levels were altered by *CTSC* expression, while KRT9 was not, indicating that CTSC may involve in the transduction of complex signaling in keratinocyte hyperkeratosis. An association between loricrin expression and cell apoptosis and proliferation was detected in vitro. Further experiments are required to confirm these associations in vivo.

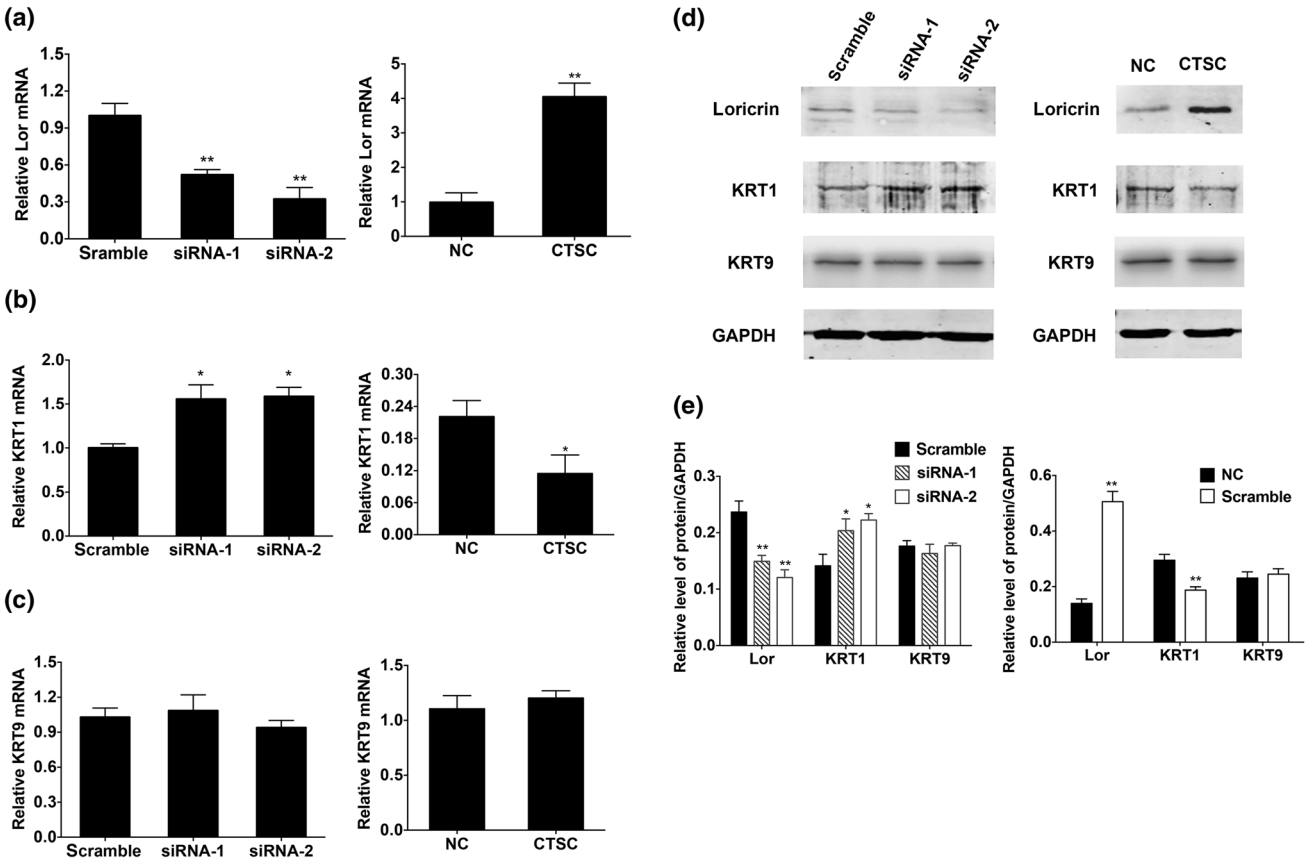

Fig. 4 Real-time PCR and Western blot analysis of HaCaT cells to assess *Lor*, *KRT1* and *KRT9* mRNA and protein expression, respectively. **a** *Lor* mRNA was increased in the CTSC-overexpression group and reduced significantly in the *CTSC*-silenced groups. **b** *KRT1* mRNA was reduced in the CTSC-overexpression group and increased in the *CTSC*-silenced groups. **c** KRT9 mRNA expression was unaffected by CTSC overexpression or silencing. **d** Western blot analysis showed that Lor, KTR1 and KRT9 protein levels correlated with mRNA expression levels. GAPDH was used as an internal protein loading control. **e** Densitometric analysis of three separate experiments. Data are presented as mean ± SD (*$P < 0.05$, **$P < 0.01$)

Conflict of interest The authors declare that they have no conflict of interest.

References

1. Gorlin RJ, Sedano H, Anderson VE (1964) The syndrome of palmar-plantar hyperkeratosis and premature periodontal destruction of the teeth. A clinical and genetic analysis of the Papillon–Lefèvre syndrome. J Pediatr 65:895–908
2. Fischer J, Blanchet-Bardon C, Prud'homme JF et al (1997) Mapping of Papillon–Lefèvre syndrome to the chromosome 11q14 region. Eur J Hum Genet (EJHG) 5:156–160
3. Laass MW, Hennies HC, Preis S et al (1997) Localisation of a gene for Papillon–Lefèvre syndrome to chromosome 11q14-q21 by homozygosity mapping. Hum Genet 101:376–382
4. Hart TC, Hart PS, Bowden DW et al (1999) Mutations of the cathepsin C gene are responsible for Papillon–Lefèvre syndrome. J Med Genet 36:881–887
5. Toomes C, James J, Wood AJ et al (1999) Loss-of-function mutations in the cathepsin C gene result in periodontal disease and palmoplantar keratosis. Nat Genet 23:421–424
6. de Haar SF, Jansen DC, Schoenmaker T et al (2004) Loss-of-function mutations in cathepsin C in two families with Papillon–Lefèvre syndrome are associated with deficiency of serine proteinases in PMNs. Hum Mutat 23:524
7. Meade JL, de Wynter EA, Brett P et al (2006) A family with Papillon–Lefèvre syndrome reveals a requirement for cathepsin C in granzyme B activation and NK cell cytolytic activity. Blood 107:3665–3668
8. Cook GP (2009) Papillon–Lefèvre syndrome and malignant melanoma. Dermatology 219:187–188
9. Pilger U, Hennies HC, Truschnegg A et al (2003) Late-onset Papillon–Lefèvre syndrome without alteration of the cathepsin C gene. J Am Acad Dermatol 49:240–243
10. Stevens HP, Kelsell DP, Bryant SP et al (1996) Linkage of an American pedigree with palmoplantar keratoderma and malignancy (palmoplantar ectodermal dysplasia type III) to 17q24. Literature survey and proposed updated classification of the keratodermas. Arch Dermatol 132:640–651
11. Reis A, Kuster W, Eckardt R et al (1992) Mapping of a gene for epidermolytic palmoplantar keratoderma to the region of the acidic keratin gene cluster at 17q12-q21. Hum Genet 90:113–116
12. McLean WH (2003) Genetic disorders of palm skin and nail. J Anat 202:133–141

13. Reis A, Hennies HC, Langbein L et al (1994) Keratin 9 gene mutations in epidermolytic palmoplantar keratoderma (EPPK). Nat Genet 6:174–179
14. Hatsell SJ, Eady RA, Wennerstrand L et al (2001) Novel splice site mutation in keratin 1 underlies mild epidermolytic palmoplantar keratoderma in three kindreds. J Invest Dermatol 116:606–609
15. Whittock NV, Smith FJ, Wan H et al (2002) Frameshift mutation in the V2 domain of human keratin 1 results in striate palmoplantar keratoderma. J Invest Dermatol 118:838–844
16. Terron-Kwiatkowski A, Paller AS, Compton J et al (2002) Two cases of primarily palmoplantar keratoderma associated with novel mutations in keratin 1. J Invest Dermatol 119:966–971
17. Terron-Kwiatkowski A, Terrinoni A, Didona B et al (2004) Atypical epidermolytic palmoplantar keratoderma presentation associated with a mutation in the keratin 1 gene. Br J Dermatol 150:1096–1103
18. Yoneda K, Demitsu T, Manabe M et al (2010) Expression of wild-type, but not mutant, loricrin causes programmed cell death in HaCaT keratinocytes. J Dermatol 37:956–964
19. Nithya S, Radhika T, Jeddy N (2015) Loricrin—an overview. J Oral Max Pathol (JOMFP) 19:64–68
20. Ishida-Yamamoto A (2003) Loricrin keratoderma: a novel disease entity characterized by nuclear accumulation of mutant loricrin. J Dermatol 31:3–8
21. Yang Y, Bai X, Liu H et al (2007) Novel mutations of cathepsin C gene in two Chinese patients with Papillon–Lefèvre syndrome. J Dent Res 86:735–738
22. Jia LF, Wei SB, Gan YH et al (2014) Expression, regulation and roles of miR-26a and MEG3 in tongue squamous cell carcinoma. Int J Cancer 135:2282–2293
23. Kosem R, Debeljak M, Repic Lampret B et al (2012) Cathepsin C gene 5′-untranslated region mutation in Papillon–Lefèvre syndrome. Dermatology 225:193–203
24. Nagy N, Valyi P, Csoma Z et al (2014) CTSC and Papillon–Lefèvre syndrome: detection of recurrent mutations in Hungarian patients, a review of published variants and database update. Mol Genet Genomic Med 2:217–228
25. Candi E, Schmidt R, Melino G (2005) The cornified envelope: a model of cell death in the skin. Nat Rev Mol Cell Biol 6:328–340
26. Hamada T, Tsuruta D, Fukuda S et al (2013) How do keratinizing disorders and blistering disorders overlap? Exp Dermatol 22:83–87
27. Bolling MC, Bladergroen RS, Van Steensel MAM et al (2010) A novel mutation in the L12 domain of keratin 1 is associated with mild epidermolytic ichthyosis. Br J Dermatol 162:875–879
28. Terron-Kwiatkowski A, van Steensel MA, van Geel M et al (2006) Mutation S233L in the 1B domain of keratin 1 causes epidermolytic palmoplantar keratoderma with "tonotubular" keratin. J Invest Dermatol 126:607–613
29. Yoneda K, Steinert PM (1993) Overexpression of human loricrin in transgenic mice produces a normal phenotype. Proc Natl Acad Sci USA 90:10754–10758
30. Jarnik M, de Viragh PA, Scharer E et al (2002) Quasi-normal cornified cell envelopes in loricrin knockout mice imply the existence of a loricrin backup system. J Invest Dermatol 118:102–109